التحليل الزلزالي الستاتيكي اللّاخطي للأنظمة الإنشائية الإطارية ذات بلاطات الجيزان المتصالبة والمدعّمة بعناصر تربيط مركزية ضخمة

د. ريم خرتش
أستاذ مساعد، قسم الهندسة الإنشائية– كلية الهندسة المدنية بالرقة– جامعة الفرات

الملخص

يتناول هذا البحث تطبيق نماذج مختلفة من عناصر التربيط القطرية الضخمة على محيط نموذج مبنى إطاري متوسط الارتفاع، مصمّم لتحمّل الأحمال الرأسية فقط، بحيث يتمكن هذا الهيكل من تحمل الأحمال الجانبية بكفاءة. يحتوي النموذج على بلاطة ذات جوائز متصالبة (متعامدة ومائلة)، لذا لا توجد أعمدة في المنتصف، مما يمنحه مرونة معمارية كبيرة.

تم في هذا البحث إضافة ستة أنواع مختلفة من أنظمة التربيط إلى نموذجي البلاطات المتصالبة (المتعامدة والمائلة) لتحمل الأحمال الجانبية، وهي: عناصر تربيط فولاذية ضخمة على شكلX، عناصر تربيط متداخلة على شكل X ، عناصر تربيط فولاذية ضخمة على شكل K، عناصر تربيط فولاذية سداسية الشكل، جدران قص خرسانية مسلحة، ونظام أعمدة خرسانية مسلحة مائلة. طُبّقت طريقة التحليل الستاتيكي اللّاخطي على النماذج الأربعة عشر باستخدام برنامج العناصر المحدودة ETABS، وحُددت نقاط الأداء بيانياً. تم الاعتماد على بيانات زلزال نورداغي في تركيا والذي حدث في 6 شباط 2023 كمنحنى طلب Demand.

أظهرت نتائج البحث أن نظام الإطار ذي عناصر التربيط الضخمة المتداخلة على شكل X أعطى سلوك جيد، حيث زادت صلابة المنشأ الجانبية عند نقطة الأداء بنسبة 331%. إضافةً إلى ذلك، أظهرت النتائج أن هذا النموذج يتمتع بأفضل أداء مع أقل عدد من المفاصل اللدن في الأعمدة مقارنةً مع النماذج الأخرى المدروسة.

الكلمات المفتاحية: عناصر التربيط المركزية الضخمة، التحليل الستاتيكي اللّاخطي، بلاطات الجيزان المتصالبة، الأحمال الزلزالية، زلزال 6 شباط 2023

Seismic Nonlinear Static Analysis of Concentric Mega Braced- Paneled Beams Frame Systems

Dr. Rim Khartash

Structural Engineering Department, Assistant Professor at Faculty of Civil Engineering in Raqqa– Al Furat University

Abstract

This paper discusses applying different configurations of mega bracings at the perimeter of a mid-height frame building model designed to sustain vertical loads merely. This will make the structure able to carry lateral loads effectively. The model has a paneled beams slab (grid and skew), so there are no columns at the middle. This will give higher architectural flexibility. In this research six different types of stiffening systems were added to the two slabs' models (grid and skew) to sustain lateral loads, i. e. mega X steel bracing, overlapping X steel bracing, mega K steel bracing, hexagon shape steel bracing, RC shear walls, and diagrid reinforced concrete system. Nonlinear static procedure was applied to the 14 models using ETABS program and the performance points were identified graphically. Where Nurdagi event - 6 February 2023 in Turkey was applied to the models as a demand curve.

The results demonstrated that Mega overlapping X braced frame system gave satisfying behavior with an increase in the structure's stiffness of 331%. Besides, the results showed that this model has the best performance with the least plastic hinges number in columns compared with the other models.

Keywords: Concentric Mega bracing, nonlinear static analysis, paneled beams slab, seismic load, 6 February 2023 Earthquakes

1. Introduction

For mid-height buildings there are four main structural systems. i.e. Frame system, Shear wall system, Dual system and interactive system. However, these systems are not capable enough to give a flexible architectural space such as galleries and shopping malls. In this research concentric mega braces are applied to a paneled beams structure with columns only on the perimeter of the building. The braces were added to the perimeter of the two

models only to sustain free space and fulfill architectural functionality. Aesthetic configurations were adopted through these six stiffening systems with glass curtain wall facades due to architectural purposes. Then a static nonlinear analysis was applied on each configuration to find out the configuration that gives the best performance under 6 February 2023 Earthquakes. Nurdagi event is scaled to zone 2B (near Aleppo) as per UBC97, [17]. Through this process several comparisons were made by different means to find an architecturally aesthetic structural solution that gives flexibility to the architect at the same time.

A lot of research were conducted about nonlinear static analysis (Pushover analysis). All of them have proved the effectiveness of this analysis procedure. (Ashwini et.al, 2024) [7], presented the origin, growth and development of pushover analysis, offering a deep insight into the attempts made by researchers in refining, redefining and enhancing pushover analysis and design of structure and its procedures. This was a detailed literature survey of nonlinear static pushover analysis from 1970 to 2023. Different researchers use pushover techniques to evaluate both existing and presumed structural behavior. The different formats of pushover analysis are also heighted along with its application on structural models to check for feasibility of various new progress in the analytical procedure. Conclusion would be in such a fashion that the Nonlinear Pushover analysis is found to be an extraordinary if it is carefully utilized by the users. Talking about capacity spectrum methods. Specifically, about determining performance points with reasonable accuracy. (Anjum et.al, 2026) [2], analyzes the behavior of a 10-story reinforced concrete (RC) building using pushover analysis (POA) and response spectrum analysis (RSA) in ETABS, following the Bangladesh National Building Code. Results indicate that while response spectrum analysis is effective for preliminary design, pushover analysis offers deeper insight into potential failure mechanisms. This study emphasizes the importance of integrating both static and dynamic approaches for a comprehensive seismic evaluation of high-rise buildings lateral load resisting system. (Guyaderand Iwan, 2004) [11], developed an improved capacity spectrum method employing statistically optimized linearization parameters. Capacity spectrum method, which is one of the three solution procedures presented in FEMA 440 as a tool of performance-based design. In this research, the researchers have developed a modified acceleration-displacement response spectrum (MADRS), which is

used in combination with the capacity spectrum designed to determine the Performance Point. Several (MADRS) are computed for several ductility values. The secant period lines are drawn for the same ductility values that is computed for the family of (MADRS). The Locus of Performance Points is created by connecting the points of intersection for each (MADRS) graph with its corresponding secant period line. The Performance Point is determined at the intersection of the Locus of Performance Points line and the capacity spectrum. Many researchers have inspected different structural systems under lateral load using static pushover analysis. (JKHSI and SABER, 2025) [15], used ASCE 7-10 and ACI 318-08 codes to design 24 buildings with different height by means of pushover analysis using ETABS software version 20.1.0. This study analyzed a dual system consisting of moment-resisting frames and shear walls. The highest stiffness factor found in low-rise buildings with smaller span lengths, higher shear wall thickness, and higher compressive strength. In comparison, the lowest stiffness factor appeared in high-rise buildings with longer span lengths, lower shear wall thickness, and lower compressive strength. However, (Mahmoud et. al, 2024) [17], used finite element models with different story numbers and seismic force resisting system configurations to find out the impact of vertically varying seismic load resisting systems through utilizing Performance-based seismic design. Two different reinforced concrete building groups that cover different heights and lateral system configurations were analyzed, group (1) includes 10 buildings with different numbers of stories (10,15,20) with both Moment-Resisting Frames at some floors and Shear Walls (at X global direction) at other ones, group (2) includes 10 buildings with different numbers of stories (10,15,20) with both Moment-Resisting Frames at some floors and Shear Walls (at both X global direction and Y global direction) at other ones. This study concluded that configuration of the lateral system in the vertical direction is sensitive and has a significant impact on the response reduction factor. When contemplating an earthquake-resistant system for a building of any height, it is preferable to use a moment-resisting floor system on the upper levels, which reduces drift, the lateral system becomes more ductile and effective in absorbing energy when it has sufficient stiffness in both directions as well. Other research tried to enhance structural system capacity by adding some elements, (Kamble, 2024) [16], studied adding steel plate shear walls and steel plate reinforced concrete composite shear walls to the structural system to improve the seismic performance of building structures. The conventional reinforced concrete shear

wall is not very ductile; it has a limited capacity to dissipate energy and is not very deformable. Specifically, the base of a typical shear wall is particularly vulnerable to earthquake damage and is highly challenging to restore. In high-rise buildings, these structural methods seem to be able to withstand lateral stresses brought on by earthquakes, blasts, and wind loads. Considering steel braces (Hadad et. al, 2014) [12], analyzed the cyclic behavior of braced concrete frames by executing an experimental investigation and numerical simulation. They made a comparison among four types of one bay RC frames: a bare frame, concrete braced frame, steel braced frame and solid bricks infilled frame. The comparisons cover the energy dissipation aspect. Experiments give the force value when the cracks start to appear and mode of failure. The energy dissipation for the braced and infilled frames is higher in comparison with the bare frame, where the increased values between 20% and 18%. Adding braces increases the lateral strength of the bare frame. The increases of lateral strength of concrete and steel bracing were 200%, 142%, respectively. However, (Bai and J, 2016) [8], have developed the Performance-Based Plastic Design (PBPD) method for the Buckling resistant braced frame system RC-BRBF. Base shear was calculated depending on energy equilibrium equation that considers energy dissipation capacity according to Large Takeda. The analyzed models were 5-10 story RC systems with Chevron bracing. The results showed that both buildings have achieved the desired level of performance in terms of Yield Mechanism, Capacity Curves, Cumulative Ductility Demands and Maximum Ductility. Considering Mega bracing system, (Abdulhameed et. al, 2023) [1], designed a multi-story steel building using ETABS software -of 52 m height- under vertical loads only. The model was enhanced with five different inner mega brace frames to carry a seismic load of El-Centro 1940 in SAP 2000 software in terms of nonlinear time history. As a result, Mega X-bracing with a diamond pattern gave the minimum roof displacement with a reduction ratio of 48%. This pattern also achieves the minimum story drift of all patterns.

The current research tries to find out a structural solution to create a column-free space. Concentric mega braces are applied to a paneled beams structure that has columns on the perimeter of the building. The plain frame model is designed to sustain merely vertical loads. Bracing system is added to carry lateral loads. The braces are added to the perimeter with different configurations. The goal is to find a structural system that makes mid-height

buildings give the best seismic performance under seismic loading with architectural flexibility without middle columns.

2. Theoretical Background

The Capacity Spectrum Method (CSM) listed in FEMA -440,[9] combines a representation of structural capacity curve with a representation of seismic demand curve to anticipate an expected displacement for a structure subjected to a specific seismic events in term of response spectrum. Structural capacity is represented by a capacity spectrum determined from a push-over analysis and seismic demand is represented by response spectra. Actually, push-over analysis represents a Shear force-Displacement curve as a result of nonlinear analysis of a building model's behaviour. The analysis depends on converting the whole structure into a single degree of freedom structure. This is executed using the first dynamic mode of the structure. This can be acceptable as a solution for low to mid rise structures. However, the results might not be correct for high rise structures which are affected with higher dynamic modes rather than the first mode only.

The Shear force-Displacement curve can be converted into a capacity curve through several procedures. Where the shear force is converted into spectral acceleration, and the displacement is converted into spectral displacement. The whole process depends on the first dynamic mode shape and the weight of the structure.

The spectral acceleration can be obtained from Eq. (1), where it is related to α_1 and W i.e. the weight of the structure. However, α_1 is calculated through Eq. (2) which is completely related to the first mode shape of the structure and the vertical distribution of the weight of the structure.

$$S_a = \frac{V/W}{\alpha_1} \tag{1}$$

Where:

$$\alpha_1 = \frac{\left(\left(\sum W_i \phi_i\right)/g\right)^2}{\left(\sum (W_i)/g\right)\left(\sum (W_i \phi_i^2)/g\right)} \tag{2}$$

The spectral displacement is calculated by Eq. (3). Where it is a function of the displacement, PF_1 factor and the maximum value of the first mode at the top of the structure.

$$S_d = \frac{\Delta}{PF_1 \phi_1} \tag{3}$$

PF_1 Factor is calculated from Eq. (4):

$$PF_1 = \frac{\sum (W_i \phi_{i1}) / g}{\sum (W_i \phi_{i1}^2) / g} \tag{4}$$

As a result the secant period of the structure at any point of the capacity curve can be calculated by Eq. (5):

$$T = 2\pi \sqrt{\frac{S_d}{S_a}} \tag{5}$$

As mentioned before finding the performance point needs a combination of the capacity curve and the demand curve which is represented by response spectrum of the studied seismic event. However, the response spectrum is given in terms of structure period rather than spectral displacement. This needs a simple modification on the response spectrum to get the spectral displacement that coincides with the spectral acceleration of it. This is done by Eq. (6)

$$S_d = S_a \left(\frac{T^2}{4\pi^2} \right) \tag{6}$$

Damping ratio of the structure at the performance point is calculated directly from capacity curve, Fig. (1). It is related to the ductility ratio Eq. (4-6) where ductility means the ability to undergo significant plastic deformation after yielding without a significant reduction in strength, the initial and second stiffness of the structure and the factor α , Eqs. (7,8,9)

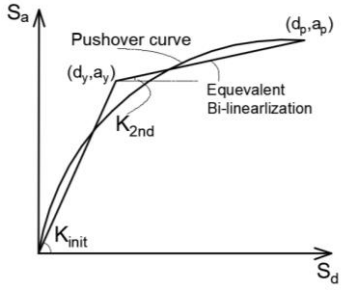


Figure.1: Capacity curve characteristics, FEMA- 440, [9]

$$\mu = \frac{d_p}{d_y} \tag{7}$$

$$K_{init} = \frac{a_y}{d_y} \qquad K_{2nd} = \frac{(a_p - a_y)}{(d_p - d_y)} \tag{8}$$

$$\alpha = \frac{K_{init}}{K_{2nd}} \tag{9}$$

$$\beta_{eff} = \beta_0 + \kappa \frac{2(\mu - 1)(1 - \alpha)}{\pi\mu(1 + \alpha\mu - \alpha)} \tag{10}$$

According to ATC-40 since $\beta_0 = 0.05 \le 0.1625$ then Hysteretic behaviour is Type A. then κ factor can be taken as $\kappa = 1$, FEMA-440,[9].

Eventually the damping ratio is given with Eq. (10). Then the equivalent period can be calculated by Eq. (11).

$$T_{\sec} = T_0 \sqrt{\frac{\mu}{(1 + \alpha\mu - \mu)}} \tag{11}$$

In order to find the performance point the procedure needs to calculate ductility ratios that coincides with the T(sec) values of the capacity curve and damping ratios as a result. This can offer a series of response spectra with different modification factors, Eq. (12). This method was explained by (Guyaderand Iwan, 2004) [11].

$$T_{eff} = T_0 \sqrt{\frac{K_i}{K_e}} \qquad M = \left(\frac{T_{eff}}{T_{\sec}}\right) \tag{12}$$

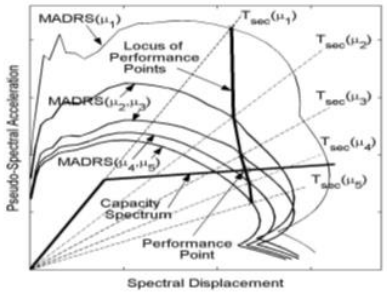


Figure.2: Determining performance point- Real events response spectra, [11]

Then a curve consists of the points of the T_{sec} lines that intersects with the response spectra would intersect with the capacity curve that represents the behaviour of the structure, Fig. (2). Considering the number and stage of the formed plastic hinges at the performance point. The stability of the structure can be determined, Fig. (3).

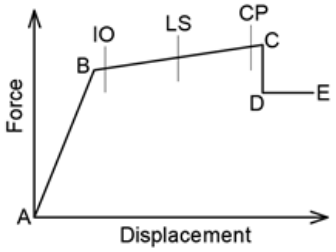
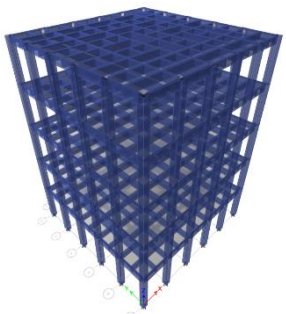


Figure. 3: Plastic Hinge curve, FEMA- 440, [9]

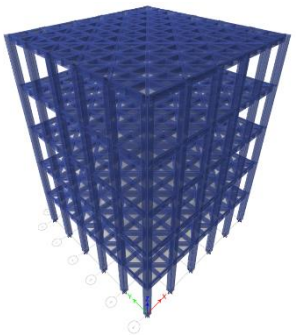
AB stage represents the linear state of the hinge. Where point B represents effective yield. However, BC stage means that the hinge gets into a non-linear stage by its ductile range. This non-linear stage is divided into three different levels: Immediate occupancy (IO): Light damage with no permanent strains, where the structure can retain original strength and stiffness. Life Safety (LS): Moderate damage with some noticeable strains which means cracks. The hinge might be beyond economical repair. Collapse Prevention (CP): High damage with large strains and cracks. The hinge is near collapse. CD stage gives a sudden reduction in load resistance followed by a reduced resistance from D to E.

3. Analyzed models

A five-story model 20x20m with a story height 5.5m, designed to carry vertical loads only. For architectural purposes no middle columns are allowed. Two slab systems were adopted, Fig. (4): the first one is a grid paneled beam slab with dimensions of 900 x 250 mm, and the second one is a skew paneled beam slab with dimensions of 600 x 250mm. Since the skew beams slab is interconnected and have less deflection, a reduced thickness of the beams is presumed, so the total weight of the two models is very close.



a. 3D – Plain Frame System- Grid paneled beam slab



b. 3D – Plain Frame System- Skew paneled beam slab

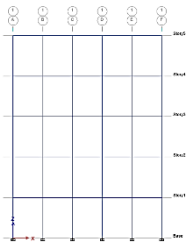
Figure. 4: Analysed models – Plain Frame

Six different types of Stiffening systems are added to the two models to sustain lateral loads i. e. mega X steel bracing, overlapping X steel bracing, mega K steel bracing, hexagon shape steel bracing, RC shear walls, and diagrid reinforced concrete bracings without columns. All these systems are added to the perimeter of the two models only to sustain free space to fulfil architectural functionality. All the models were built in ETABS 20.1.0, and nonlinear static pushover analysis was applied to all of them, where P-delta effect was checked for all models.

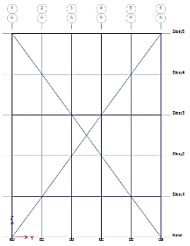
Live load equals 3 kN/m^2, flooring load equals 2 kN/m^2. Steel bracings have a section of HS: 100 x 200 x 10 and steel grade of S355. RC Longitudinal reinforcement f_y=400MPa, Shear reinforcement f_y=280MPa. A higher characteristic compressive strength was adopted for stiffening shear walls and diagrid bracings with f'_c=28MPa, where the rest elements have a value of f'_c=25MPa for characteristic compressive strength. Expected yield strength which is considered in backbone curve: (f_{ye}) is taken 1.25 times the nominal yield strength (f_y) for braces and reinforcement. Expected compressive concrete strength (f'_{ce}) equals 1.3 times the lower-bound compressive strength (f'_c=25MPa) as per ASCE 41-14, [6].

Concrete bracings have a section of 300x600 mm with $12T20, \phi 10/15cm$ reinforcement. Fig. (5) Depicts the six different configurations of the stiffening systems added to plain frame models to sustain seismic loads. Four of them are steel mega bracings. Diagrid and shear wall systems are made of reinforced

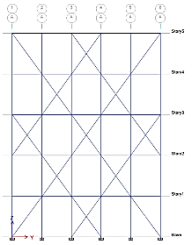
concrete. All of them are added to the perimeter of the structure. The braces are added to the four sides of the models symmetrically.



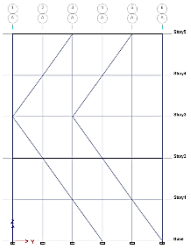
a. Plain Frame system



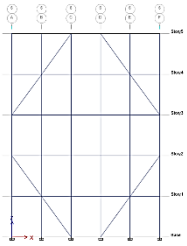
b. Mega X bracing



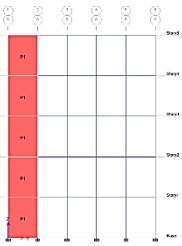
c. Overlapping X



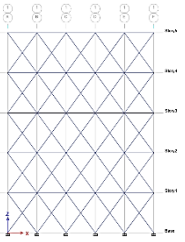
d. Mega K bracings



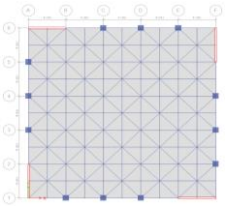
e. Hexagon shape bracing



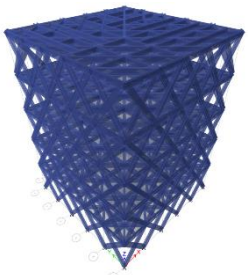
f. Shear wall



g. RC DiaGrid bracing



h. shear wall distribution



k. 3D shape- RC DiaGrid bracing

Figure. 5: Bracing and stiffening systems

Plastic hinges backbone curves were defined automatically in ETABS as per ASCE 41-13, [5]. Beams hinges defined as table 10-7: concrete beams-flexure. M_3 degree of freedom at the beginning and end of beams. Column hinges as table 10-8: concrete columns. P-M_2-M_3 degree of freedom at the beginning and end of columns. Steel braces hinges as table 9-7. Axial (P) at the beginning and end of beams. Shear wall hinges: auto fiber (P-M_3).

Nurdagi event was applied to the models as a demand curve. It took place on 6 February 2023 in Turkey near Gaziantep with 21.27km distance of epicentre. PGA was 1.35m/sec^2. With (S_c) soil type, shear wave velocity was 599 m/s. The response spectrum is scaled to a target spectrum in zone 2B as per UBC97 code, [15] by a scale factor SF= 0.581. Scaling was done according to amplitude scaling method as per ASCE7-16, [4]- section 16.2.3. Where Average spectral ratio scaling procedure was adopted within a period range $0.2T_1$ to $1.5T_1$, ASCE7-16, [4]- section 21.2, where T_1 is the fundamental period of the structure. Since the models have different period values, the minimum and maximum fundamental periods of models were adopted. Directionality SRSS of the pairs EW, NS was adopted. Then the response spectrum is converted to spectral coordinates S_d-S_a, Eq(6)- Fig. (6,7).

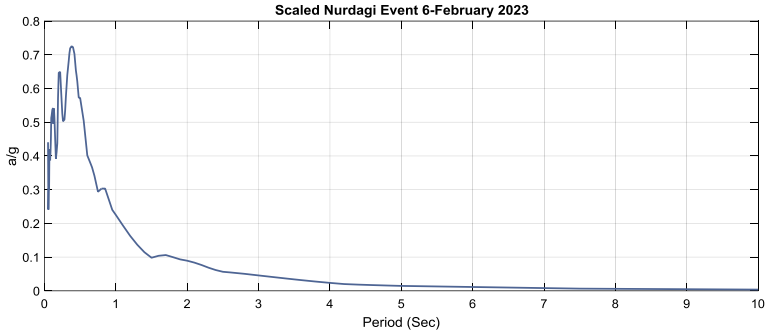


Figure.6 Nurdagi event's Response Spectrum

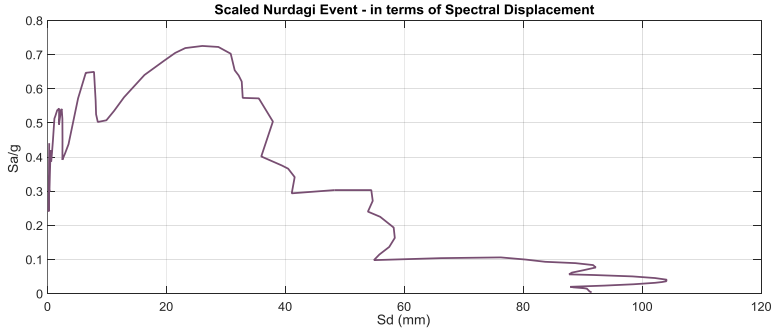
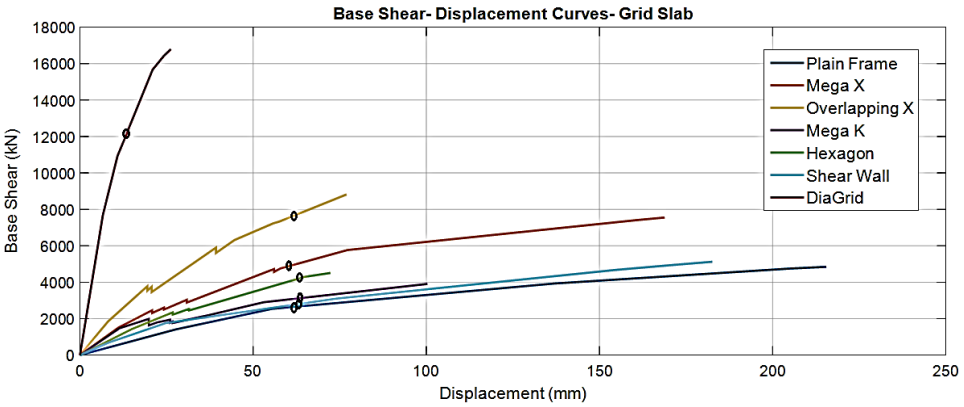


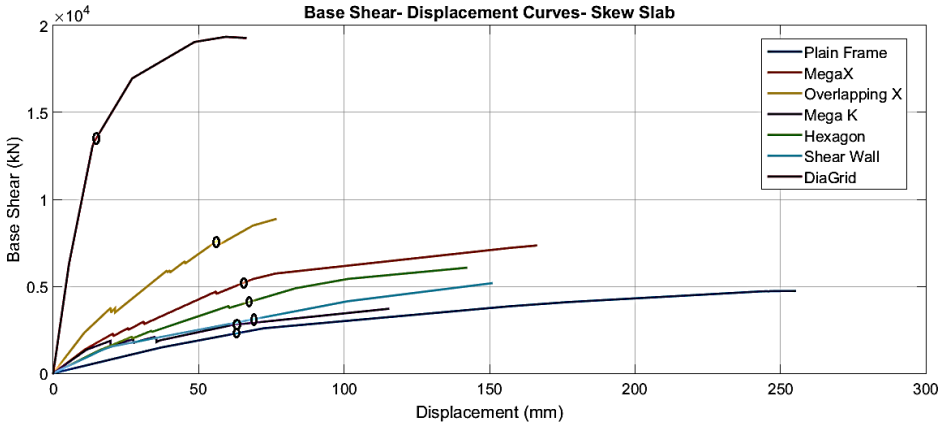
Figure.7 Nurdagi event's Spectral coordinates, (Eq. 6)

4. Analysis results

After defining the plastic hinges and applying nonlinear analysis to the 14 models. The shear force- displacement curves were obtained, Fig. (8) From which the most ductile model is the plain frame system sustains the maximum displacement. However, the plain frame models have the lowest value of base shear. Fig. (8) Also shows that all models fulfil the condition $\mu_{strength} < \mu_{\max}$, $ASCE7-16$,[4]. Except for grid slab model-DiaGrid. In general, all skew slab models gave better results than grid slab model. Which is probably due to the additional stiffness gained by beams interconnections.



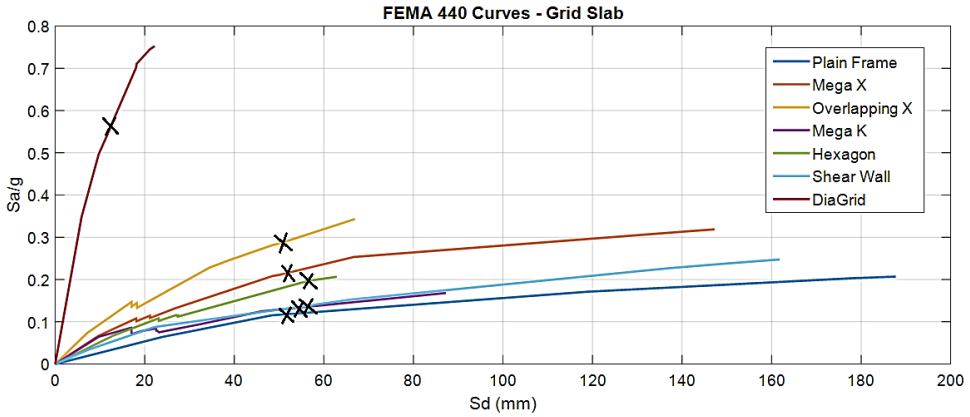
a. The shear force- displacement curves Grid Slab



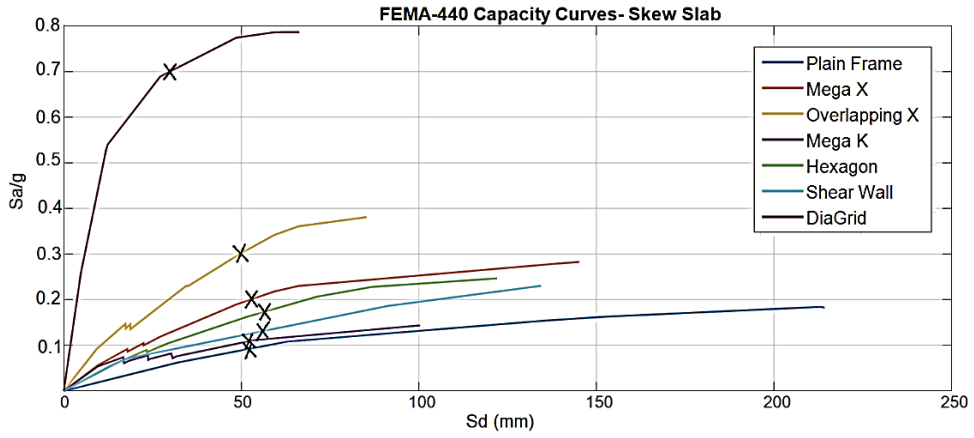
b. The shear force- displacement curves Skew Slab

Figure.8 The shear force- displacement curves of 14 models

After converting the curves into capacity curves by converting displacement into spectral displacement. A set of curves are obtained as per FEMA-440, [9], Fig. (9).



a. The Capacity curves Grid Slab



b. The Capacity curves Skew Slab, (Eq. 1,3)

Figure.9 The Capacity curves of 14 model

By intersecting demand curve with capacity curve, the performance point could be identified i.e. Nurdagi event's Response spectra –scaled to zone 2B as per UBC97 with the FEMA-440 capacity curve, Fig. (10). performance

points are obtained for all 14 models. The adopted procedure was to calculate values of ductility μ that coincides with T_{sec} values of the capacity curve of the model, Eq. (11). And calculating modification factors, Eq. (12) and obtaining a set of modified demand curves. Each of them will intersect with the period lines by a point. The series of points will make a curve that intersects with the capacity curve of the model identifying the performance point.

Table. 1 Ductility value and modification factor according to T_{sec} of Overlapping X braced frame model's capacity curve

T_{sec}	MF, (Eq. 12)	μ (*Eq.*11)
0.64	1.56	0.66
0.69	1.36	0.84
0.70	1.29	0.92
0.72	1.24	1.00
0.75	1.15	1.19
0.82	0.96	1.88
0.89	0.82	3.41

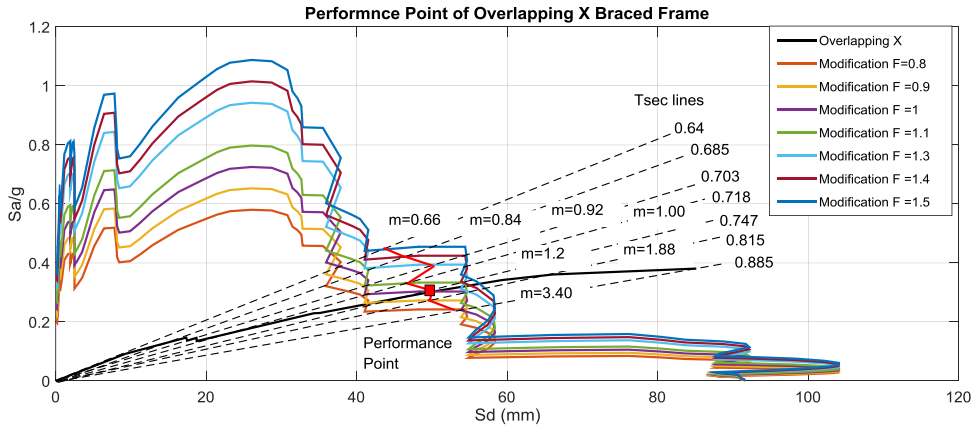


Figure. 10 Finding performance point of overlapping X Supporting system

The performance points parameters of the 14 models are tabulated in table. (2). Although all the models have approximately similar weight values the dynamic properties of them are different. i. e. fundamental period. It has a range from

0.306 sec to 1.418 sec. From which it can be said that the difference in configurations makes a big change in dynamic properties.

Table.2 Performance point parameters, Fig. (9)

Grid Slab

System	Plain Frame	Mega X	Overlapping X	Mega K	Hexagon	Shear wall	DiaGrid
S_d (mm) (Eq.3)	56	55	54	58	58	57	13
S_a (/g) (Eq.1)	0.12	0.22	0.3	0.135	0.2	0.14	0.57
T_{eff} (Eq.12)	1.72	1.04	0.81	1.20	1.23	1.25	0.35
T_0 (ETABS)	1.35	0.94	0.72	0.97	1.15	1.22	0.32
W (kN)	30721.1	30826.4	30955	30826.5	30803.1	30857.4	31561.9
T_{sec} (ETABS)	1.50	1.05	0.82	1.35	1.17	1.30	0.42
M F (Eq.12)	1.31	0.98	0.97	0.79	1.10	0.93	0.70
α (Eq.9)	0.81	0.57	0.51	0.26	0.67	0.43	0.32
μ (Eq.7)	1.70	3.18	2.90	3.21	2.46	3.32	2.61
κ (Fig.2)	1.00	0.80	0.80	0.78	0.82	0.78	0.81

β% (Eq.10)	0.08	0.12	0.13	0.21	0.10	0.15	0.19

Skew Slab

System	Plain Frame	Mega X	Overlapping X	Mega K	Hexagon	Shear wall	DiaGrid
S_d (mm) (Eq.3)	54.88	57	50	55	58	59	30.5
S_a (/g) (Eq.1)	0.0982	0.215	0.3	0.12	0.18	0.14	0.7
T_{eff} (Eq.12)	1.89	0.97	0.80	1.12	1.11	1.12	0.35
T_0 (ETABS)	1.42	0.87	0.67	0.89	1.04	0.80	0.31
W (kN)	28273.4	28378.8	28507.6	28378.8	28355.4	30748.4	29008.6
T_{sec} (ETABS)	1.43	0.99	0.85	1.30	1.10	1.10	0.32
M F (Eq.12)	1.75	0.95	0.89	0.74	1.02	1.03	1.23
α (Eq.9)	0.65	0.49	0.45	0.22	0.57	0.46	0.53
μ (Eq.7)	2.33	3.04	3.31	3.36	2.49	2.65	2.27
κ (Fig.2)	0.83	0.78	0.78	0.78	0.82	0.81	0.88
β% (Eq.10)	0.11	0.14	0.14	0.23	0.12	0.15	0.14

By returning to the base shear- displacement curves, displacement values at the performance point can be obtained. Table. (3). Shows the step of the performance point.

Table.3 Performance Point's displacements in (mm) and base shear in (kN).

Performance Point's displacements and base shear

Slab Type		Plain Frame	Mega X	Overlapping X	Mega K	Hexagon	Shear wall	DiaGrid
Grid Slab	Step	10	10	10	11	9	3	5
	Displ.	64.36	63.22	64.36	66.67	66.67	65.53	13.76
	V kN	2693	5034	7852	3190	4300	2868	12299
Skew slab	Step	10	10	13	13	8	4	5
	Displ.	63.08	65.53	57.47	63.22	66.67	67.82	13.96
	V kN	2320	5400	7683	2778	4580	3044	13284

Plastic hinge analysis at the final step is shown in table. (4) where the number of plastic hinges is shown, the stage and the correlated element are tabulated. The best behavior goes to the Overlapping X stiffening system for a skew paneled beam slab where it has at the performance point: 12 plastic hinges- stage IO in braces and 2 plastic hinges-CP stage in columns. While the plain Frame model has 14 plastic hinges- stage IO in columns and 2 plastic hinges-CP stage in columns as well, Fig. (11). It is obvious that there are no plastic hinges in the paneled beams slab. Which means that the model succeeded in making an architectural free space that resists lateral force as well.

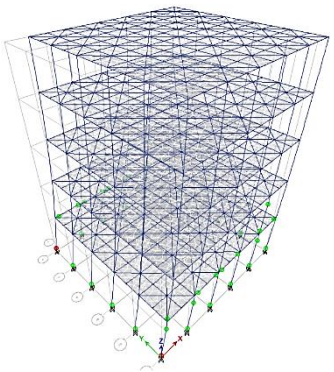
Table.4 Plastic hinge analysis

Final Step's plastic hinges

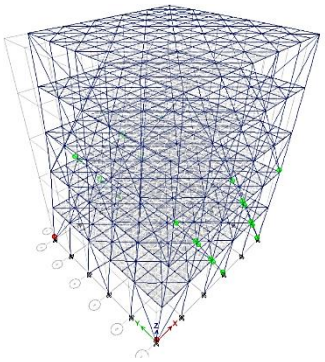
Slab Type	Plain Frame	Mega X	Overlapping X	Mega K	Hexagon	Shear wall	DiaGrid
Grid Slab	40 IO Beam	16 IO Br	16 IO Br	12 IO Br	6 IO Br	14 IO Br	14 CP Br

	20 IO Col	16 IO Col 4 CP Col	2 CP Col	14 IO Col	12 IO Col	6 IO Col	
	4 CP Col	12 IO Beam		2 CP Col	2 CP Col	2 CP Col	
Skew slab	34 IO Col	12 IO Br	14 IO Br	12 IO Br	6 IO Br	10 IO Br	8 CP Br
	2 CP Col	18 IO Col 2 CP Col	2 CP Col	14 IO Col	12 IO Col	6 IO Col	
		2 IO Beam		2 CP Col	2 CP Col	1 CP Col	

Br: braces, Col: Column



a. Plastic hinges-plain frame at the Performance point



b. plastic hinges- overlapping X at Performance point

Figure. 11: Plastic hinges at performance point's step for plain frame and overlapping X bracing

Table. (5) shows the response modification factor of R for all 14 models. Which varies depending on the nonlinear behavior of the structural system. Where $R = R_{\mu} \times R_s$; $R_{\mu} = V_e / V_u$ and $R_s = V_u / V_d$, ASCE7-16, [4].

V_e: Elastic strength
V_u: actual strength
V_d: design strength

Table.5 Response modification factor

Grid Slab	Plain Frame	Mega X	Overlapping X	Mega K	Hexagon	Shear wall	DiaGrid
R	5.5	8.4	7.15	4.706	4.118	5.6	3.625
Skew Slab	Plain Frame	Mega X	Overlapping X	Mega K	Hexagon	Shear wall	DiaGrid
R	5.25	7.826	7.5	5.25	5	6	5.077

5. Conclusion

Inspecting all parameters, the skew paneled beam slab gave better performance than the grid slab. Where the slab acts as horizontal diaphragm that transfers lateral loads to the seismic resisting system. The bi- directional interaction significantly alters the force distribution and stiffness of the seismic resisting system. Firstly, considering lateral stiffness mega brace systems increased the lateral stiffness with a noticeable ratio. The diagrid RC system and the overlapping X braces frame system has the maximum amplification ratio with a value of 573% and 331% respectively. Which was proved by (Hadad, 2014) [10] and (Abdulhameed et. al, 2023) [1]. Hence, the two systems sustain the least values of top displacement with a reduction of 22% and 91% respectively. Secondly, considering plastic hinge analysis it is obvious the overlapping X braced frame system gave the optimum performance, since the hinges were mostly in braces (14-16 hinges) while only two columns were damaged. Which is very good since most of the columns are safe and the rehabilitation can be done easily. The plain frame system would

have 24 column hinges and 40 beam hinges at the final step for grid slab. While it would have 36 column hinges and no beam hinge at the final step for skew slab. The shear wall frame system gave 14 hinges in beams and 8 hinges in columns for grid slab, and it gave 10 hinges in beams and 7 hinges in columns for skew slab at final step. Furthermore, in terms of response modification factor the Mega X bracing frame system and the overlapping X bracing frame system have the highest values between 7.15-8.4 for grid slab and skew slab as well. Finally, the shear wall frame and diagrid systems have more like elastic behaviour since they have less ductility than the other systems, as it was proved by (Kamble, 2024) [16]. However, at the performance point for grid slab the most ductile systems are the overlapping X and mega X braced frame systems with 3.3% and 3.36% ductility ratios. For skew slab the most ductile systems are the mega X, overlapping X and mega K braced frame systems with 3.18%, 2.9% and 3.21% ductility ratios.

As an extend to this topic an eccentric bracing system can be considered since they can dissipate energy through ductility more effectively than concentric braces. Concentric mega bracing with ductile shear links can be analyzed using NSP (Nonlinear Static Procedure) to find out the best solution. Soil type effect can be considered to find out the best configuration for each soil type.

6. References

1. Abdulhameed. A, Ahmad. M, Karim. A, 2023. *Enhancing Seismic Performance Of Multi-Story Steel Buildings Using Inner Mega Braced Frames.* Basra, Iraq: Misan Journal of Engineering Sciences.
2. Anjum. N, Rana. M, Islam. F, Rahman. M, 2026. *Seismic Performance Evaluation of a 10-story RC Building Using Pushover Analysis & Response Spectrum Analysis.* Bangladesh: American Journal of Civil Engineering.
3. *Disaster and Emergency Management Autority (AFAD).* Turkey: 2023.
4. ASCE7-16, 2016. *American Society of Civil Engineering.* USA.
5. ASCE 41-13, 2013. *American Society of Civil Engineering*. USA.
6. ASCE 41-14, 2014. *American Society of Civil Engineering*. USA
7. Ashwini .L. K, Keshavamurthy. M, Ravikumar. C, 2024. *Pushover Analysis -A Review.* Bengaluru, India: JETIR.

8. Bai. J and J. Ou, 2016. *Earthquake-Resistant Design Of Buckling-Restrained Braced Rc Moment Frames Using Performance-Based Plastic Design Method.* s.l.:Engineering structures.
9. FEMA-440, *Federal Emergency Management Agency*. US.
10. Genikomsou. A, 2024. *Seismic Damage Assessment Of Reinforced Concrete Slacolumn Connections—Review Of Test Data, Code Provisions And Analytical Models.* Canada: MDPI.
11. Guyader. A, and Iwan.W, 2004. *An Improved Capcity Spectrum Method Employing Statistically Optimized Linearization Parameters.* Canada: 13th World Conference on Earthquake Engineering.
12. Hadad. H, Metwally. I, El-Betar. S, 2014. *Cyclic Behavior Of Braced Concrete Frames.* Cairo: HBRC Journal.
13. CSI Incorporation., *ETABS. 20.0.0.*
14. JKHSI.S, and SABER. S, 2025. *Factors Influencing The Elastic Stiffness Factor In Reinforced Concrete Structure Of Dual System Using Pushover Analysis.* Northern Cyprus: IIUM Engineering Journal.
15. Kamble. D, 2024. *A Conceptual study of Wind Load with Different Types of Lateral Load Resisting Methods in 15-Storey Structure*. s.l.:Interantional Journal Of Scientific Research In Engineering And Management.
16. UBC97, 1997. *UNIFORM BUILDING CODE*
17. Mahmoud. O, El-Kateb. M, Zaher. A, 2024. *Performance-Based Seismic Analysis of RC Structures with Vertically Variable Lateral Load Resisting System.* Cairo: IJCRT.